THE JOURNAL OF PHYSICAL CHEMISTRY A

Article

pubs.acs.org/JPCA

Spectroscopic and Computational Characterization of the HCO···H_2O Complex

Qian Cao,[†] Slawomir Berski,[‡] Markku Räsänen,[†] Zdzislaw Latajka,[‡] and Leonid Khriachtchev*[,†]

[†]Department of Chemistry, P.O. Box 55, FIN-00014, University of Helsinki, Finland

[‡]Faculty of Chemistry, University of Wroclaw, 14, F. Joliot-Curie Str., 50-383 Wroclaw, Poland

Supporting Information

ABSTRACT: The complexes of HCO with water are prepared in a Kr matrix and characterized by IR spectroscopy with the aid of ab initio calculations. The calculations at the UCCSD(T)/aug-cc-pVTZ level of theory predict three structures of the HCO···H_2O complex. In the "linear" structure **I**, a hydrogen atom of water interacts with the oxygen atom of HCO. In structure **II**, the hydrogen atom of HCO interacts with the oxygen atom of water. The "cyclic" structure **III** has the C−H···O and O−H···O hydrogen bonds simultaneously. In the experiment, the HCO···H_2O complex is produced by photolysis of HCOOH/HY/Kr (Y = Br and Cl) matrices followed by thermal annealing at about 30 K, which promotes the H + CO···H_2O → HCO···H_2O reaction. The analysis of the spectroscopic data shows that the main product has structure **III** whereas the formation of structure **II** is less efficient. The experiments show no evidence of the weakest structure **I**. The experiments with deuterated formic acid (DCOOH) provide additional support of the proposed assignment.

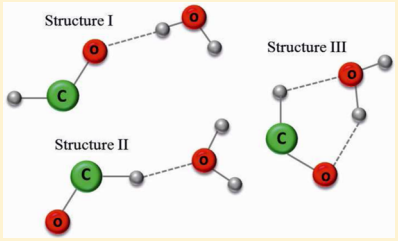

INTRODUCTION

Noncovalent interactions are crucial for understanding structures and properties of matter and many physical, chemical, and biological processes in nature.[1,2] Since water is an important component in the Earth's atmosphere, hydrogen-bonded water complexes with other molecules have been extensively investigated.[3,4] On the other hand, complexes between water and radicals have been studied less, despite their importance in atmospheric chemistry.[5] The complexes of water with hydroxyl (OH) and hydroperoxyl (HO_2) radicals are prototype radical−molecule complexes, which have been studied both theoretically and experimentally.[4,5] The water complexes of other radicals, such as nitric oxide (NO),[6] chlorine dioxide (OClO and ClOO),[7,8] nitrogen dioxide (NO_2),[9] and chlorine oxide (ClO),[10] have also been studied with respect to atmospheric chemistry. It is essential that bonding with water may affect the reactivity of the radical. For example, the presence of water enhances the rate constant of the HO_2 self-reaction.[11] Similar enhancement is also seen in the reaction between HO_2 and NO_2.[12] The effect of coadsorbed water on the stability and configuration of the methanol electro-oxidation intermediates (HCO and COH) on platinum (111) has recently been reported.[13]

The formyl radical (HCO) has attracted considerable attention due to its role in astrophysics, hydrocarbon combustion process, and photochemistry of the terrestrial troposphere.[14] The formation of HCO in the gas-phase is possibly the first key step in the synthesis of organic species such as carboxylic acids, aldehydes, and alcohols in cold interstellar clouds.[15] This H + CO → HCO reaction has been studied computationally[16] and experimentally.[17,18] The properties of HCO have been the subject of several spectroscopic[19−21] and theoretical[22,23] investigations. However, to our knowledge, the complex of HCO with water has not been studied in detail.

Matrix isolation is a powerful method for spectroscopic studies of reactive species, and IR spectra of numerous free radicals trapped in noble gas matrices have been reported. The formyl radical was the first polyatomic radical stabilized in a cryogenic matrix in sufficient concentration. The first IR spectroscopic study of HCO in a solid matrix was performed in 1960 by Ewing et al. using photolysis of HI and HBr in a CO matrix.[24] The formation of HCO from H and CO was observed at 3 K, indicating a very low reaction barrier.[18] Complexes of water with a number of open-shell species have been studied in matrices, for example, with nitric oxide (NO),[6] OClO,[7] OH,[25,26] HO_2,[27] phenyl,[28] and phenoxyl[29,30] radicals.

A number of methods can be used to prepare intermolecular complexes in cryogenic matrices. The complexes are often prepared by adding two species to the matrix gas and depositing the matrix at somewhat elevated temperatures and/or annealing the matrix after deposition. However, this general strategy seems to be less suitable for radicals that are difficult to prepare in the gas phase. In addition, this method leads to relatively small amounts of the 1:1 complexes with an interference of monomers and larger clusters. A more sophisticated approach is based on photolysis of proper precursors isolated in a matrix. For example, photolysis of formaldoxime leads to the formation of the HCN···H_2O and HNC···H_2O complexes[31] and that of H_2O_2 produces the O···H_2O complex.[32] Propiolic acid photodissociates producing

Received: January 28, 2013
Revised: April 3, 2013
Published: April 25, 2013

a number of complexes, including one between water and C_3O.[33] As an important observation, photolysis of formic acid efficiently produces a complex between water and CO.[34] Another interesting possibility is to obtain a small fragment by photolysis and mobilize this fragment by annealing, producing a complex of this fragment with another molecule. This approach has been used to prepare the O···H_2O[35] and O···*cis*-HCOOH[36] complexes, the O atoms being released from N_2O. The mobile fragment can also chemically react with some complex in the matrix, hence producing another complex. In this way, intermolecular complexes of noble-gas hydrides HNgY···X have been prepared.[37]

In the present work, we study the HCO···H_2O complex by IR spectroscopy in a Kr matrix. In order to prepare this complex, an unusual "double photolysis" approach is used. We start with HBr (or HCl) and HCOOH isolated in a Kr matrix. Upon 193 nm photolysis, HCOOH dissociates to the CO···H_2O complex, and H atoms are produced from HBr. Thermal mobilization of the H atoms promotes the H + CO···H_2O reaction, leading to the formation of the HCO···H_2O complex. The structural assignment is based on calculations at the UCCSD(T) and UMP2 levels of theory.

COMPUTATIONAL DETAILS AND RESULTS

Computational Details. The optimization of the structures and calculation of the relative energies and vibrational spectra were performed at the UCCSD(T)/aug-cc-pVTZ level of theory using the *MOLPRO* program[38] and at the UMP2/aug-cc-pVTZ using the *Gaussian09* program.[39] The minima on the potential energy surface were verified by analysis of the harmonic vibrations which yielded no imaginary frequencies. The interaction energy (E_{int}) of the HCO···H_2O complexes was obtained as the total energy (E_{tot}) difference between the complex and the HCO and H_2O monomers with structures corresponding to the complex. The value of E_{int} was corrected (E_{int}^{CP}) by the basis set superposition error (BSSE) using the counterpoise procedure.[40] Additionally, the value of E_{int}^{CP} was corrected for vibrational zero-point energy (ΔZPVE). The natural population analysis (NPA)[41] was carried out using the *Gaussian09* program (version C.01) and the post-Hartree–Fock density calculated at the UCCSD/aug-cc-pVTZ//UCCSD(T)/aug-cc-pVTZ level of theory.

Computational Results. The optimization of the geometrical structures of the HCO···H_2O complex at the UCCSD(T)/aug-cc-pVTZ level yields three energy minima on the potential energy surface (Figure 1). For these structures, the spin contamination is below 3%. It follows that the mixing of different electronic spin states with the ground state is very small, and the unrestricted form of orbital-based wave function is a reasonable approximation. The geometrical parameters of these structures are presented in Table S1.

The lowest total energy at the UCCSD(T) level is found for the cyclic form (structure **III**), which is formed by the intermolecular C–H···O and O–H···O bonds. The total energy of this structure is lower than those of the linear structures **I** and **II** by 1.04 and 0.78 kcal mol^{-1}. However, after accounting for zero-point vibrational energy (ΔE_{tot} + ΔZPVE), the order of stability is changed (Table 1), and structure **II** with one C–H···O hydrogen bond becomes the most energetically favorable. The strongest intermolecular interactions with BSSE and ZPVE corrections (E_{int}^{CP} + ΔZPVE) are found for structures **II** (−1.70 kcal mol^{-1}) and **III** (−1.61 kcal mol^{-1}) while structure **I** is the weakest complex (−0.83 kcal mol^{-1}, Table 1).

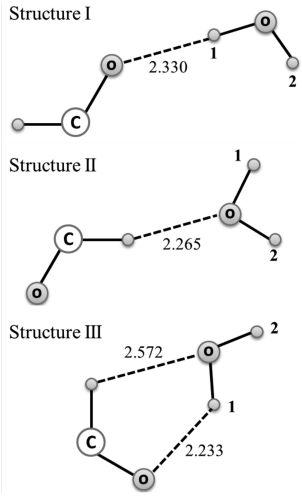

Figure 1. UCCSD(T)/aug-cc-pVTZ optimized structures of the HCO···H_2O complex with intermolecular bond lengths (in Å).

Table 1. Calculated Energies (in kcal mol^{-1}) of the HCO···H_2O and the HCO···HOD Complexes at the UCCSD(T)/aug-cc-pVTZ Level of Theory

	Structure I	Structure II	Structure III
	HCO···H_2O		
ΔE_{tot} + ΔZPVE	0.75	0.00	0.04
E_{int}	−2.64	−2.92	−3.71
E_{int}^{CP}	−2.24	−2.62	−3.35
BSSE	0.40	0.30	0.36
E_{int}^{CP} + ΔZPVE	−0.83	−1.70	−1.61
ΔZPVE	1.41	0.92	1.74
	HCO···HOD		
E_{int}^{CP} + ΔZPVE	−1.10[a]	−1.69[a]	−1.94[a]
	−0.96[b]	−1.70[b]	−1.79[b]
ΔZPVE	1.14[a]	0.93[a]	1.41[a]
	1.28[b]	0.92[b]	1.56[b]

[a]D atom in position 1 (Figure 1). [b]D atom in position 2 (Figure 1).

The changes of the intramolecular bond lengths upon complexation are very small (Table S1), which is typical for noncovalent interactions. In the case of structures **II** and **III**, very small shortening of the CH bond is observed due to its hydrogen bonding with the water O atom (by 0.004 and 0003 Å, respectively), and the water O–H bond participating in the hydrogen bond in structure **III** is elongated by 0.002 Å. In structure **I**, the water O–H bond participating in the hydrogen bond is slightly elongated (+0.001 Å) whereas the other O–H bond is slightly shortened (−0.001 Å).

The NPA results confirm that the complexes may be viewed as formed by the HCO radical and H_2O molecule. The unpaired electron is localized entirely at the HCO molecule with the largest value of the spin density at the C atom (0.7 e). The probability of finding the unpaired electron at the H and O atoms is much smaller with the spin densities of 0.1 and 0.2 e, respectively.

The characteristic frequencies of the complexes obtained in the harmonic approximation at the UCCSD(T)/aug-cc-pVTZ level of theory are presented in Table 2 (HCO···H_2O) and in Table 3 (HCO···HOD). The full spectra at the UCCSD(T)/

dx.doi.org/10.1021/jp4009477 | J. Phys. Chem. A 2013, 117, 4385–4393

Table 2. Frequencies and Shifts (ω and $\Delta\omega$, in cm^{-1}) of the HCO and H_2O Monomers and HCO···H_2O Complexes

	experiment				calculation[a]			
	monomer	complex			monomer	I	II	III
mode	ω	ω	$\Delta\omega$	assign.	ω	$\Delta\omega$	$\Delta\omega$	$\Delta\omega$
				H_2O				
ν_{as}OH	3723.5[b]	3734.6	+11.1	II	3919.39	−10.6	−2.7	−11.3
		3725.3	+2.2	III				
		3723.1	−0.4	III				
ν_{sym}OH	3627.6[b]	3627.8	+0.2	III	3810.23	−8.5	−1.9	−18.6
		3626.8	−0.8	III				
δHOH	1586.4[b]	1590.8	+4.4	III	1645.33	+11.8	+1.0	−0.9
		1588.8	+2.4	III				
				HCO				
νCH	2467.1	2530.5	+63.4	III	2704.24	+33.0	+89.3	+64.9
		2523.8	+56.7	III				
νC═O	1860.3	1858.8	−1.5	I or II[c]	1876.40	−3.4	−11.1	−10.6
		1855.6	−4.7	III				
		1853.3	−7.0	III				
		1850.6	−9.7	II				
δHCO	1081.2	1097.7	+16.5	III	1107.24	+10.4	+36.7	+17.5
		1096.6	+15.4	III				

[a]The calculations were done at the UCCSD(T)/aug-cc-pVTZ level of theory. [b]VR origin for HOD in a Kr matrix.[61] [c]Tentative assignment.

Table 3. Frequencies and Shifts (ω and $\Delta\omega$, in cm^{-1}) of the HCO and HOD Monomers and HCO···HOD Complexes

	experiment				calculation[a]						
	monomer	complex			monomer	I[c]	I[d]	II[c]	II[d]	III[c]	III[d]
mode	ω	ω	$\Delta\omega$	assign.	ω	$\Delta\omega$	$\Delta\omega$	$\Delta\omega$	$\Delta\omega$	$\Delta\omega$	$\Delta\omega$
					HOD						
νOH	3677.1[b]	3693.0	+15.9	III[c]	3867.30	+3.4	−22.6	−2.1	−3.0	+5.5	−37.7
νOD	2702.4[b]	2691.6	−7.1	III[c]	2807.33	−15.9	+3.2	−1.6	−1.0	−26.7	+4.9
		2688.5	−10.8	III[c]							
δHOD	1396.7[b]	1394.5	−2.2	III[c]	1442.36	−1.4	+22.6	+1.9	+1.4	−9.2	+8.3
					HCO						
νCH	2467.1	2531.8	+64.7	III[c]	2704.24	+34.4	+34.6	+89.1	+89.1	+63.4	+63.8
		2524.8	+57.7	III[c]							
νC═O	1860.3	1858.7	−1.6	I or II[e]	1876.40	−2.8	−2.8	−11.1	−11.1	−10.1	−10.9
		1855.1	−5.2	III[c]							
		1852.7	−7.6	III[c]							
		1850.5	−9.8	II[e]							
δHCO	1081.2	1097.9	+16.7	III[c]	1107.24	+8.1	+8.1	+36.4	+36.5	+13.9	+15.8
		1097.0	+15.8	III[c]							

[a]Calculations were done at the UCCSD(T)/aug-cc-pVTZ level of theory. [b]VR origin for HOD in a Kr matrix.[61] [c]D atom in position 1 (Figure 1). [d]D atom in position 2 (Figure 1). [e]Tentative assignment is done is analogy with the HCO···H_2O complex.

aug-cc-pVTZ and UMP2/aug-cc-pVTZ levels are presented in Table S2 and in Table S3.

EXPERIMENTAL DETAILS AND RESULTS

Experimental Details. Formic acid (FA, HCOOH, 99%, Kebo Lab and DCOOH, 99%, Icon Isotopes) was purified by several freeze−pump−thaw cycles. HBr (≥99%, Aldrich), HCl (≥99%, Linde), CO (≥99.95%, AGA), and Kr (≥99.999%, AGA) gases were used as supplied. The FA/HY/Kr (Y = Cl, Br) gas mixtures with the concentration ratios of ∼1/2/1000 were prepared by mixing the gases in a glass bulb and deposited onto a CsI window at 20 K in a closed cycle helium cryostat (RDK−408D, Sumitomo Heavy Industries). CO/HBr/Kr (1/2/1000) matrices were studied under the same experimental conditions for comparison. The spectra in the 4000−500 cm^{-1} region (resolution of 0.5 cm^{-1}) were recorded at 4.3 K using a Bruker VERTEX 80 FTIR spectrometer coadding typically 200 scans. The matrices were photolyzed at 4.3 K with a 193 nm ArF excimer laser (MSX-250, MPB, pulse duration of ∼10 ns, and pulse energy density of ∼10 mJ cm^{-2}). A continuous-wave Ar-ion laser (Omnichrome 543-AP) operating at 488 nm (intensity of ∼10 mW cm^{-2}) was used to decompose annealing-induced products.

Experimental Results. The IR spectra of HCOOH and DCOOH in low-temperature matrices have been previously studied.[34,42] The vibrational bands of HCOOH and DCOOH in a Kr matrix observed in the present work are shown in Table S4. The observed splitting of the vibrational bands is presumably due to different trapping sites in a Kr matrix. For FA/HY/Kr (1/2/1000, Y = Cl and Br) matrices deposited at 20 K, the FA monomer bands dominate over the dimer bands. HCl (2872.6 and 2870.7 cm^{-1}) and HBr (2551.4 cm^{-1}) are

dx.doi.org/10.1021/jp4009477 | J. Phys. Chem. A 2013, 117, 4385−4393

also mostly monomeric in these matrices and the bands of HCl (2815.1 cm^{-1}) and HBr (2491.6 cm^{-1}) dimers are weak. For a CO/HBr/Kr (1/2/1000) matrix, the CO monomer band is located at 2135.5 cm^{-1}, in agreement with the literature data,[43] and the HBr···CO complex is also observed in the HBr (2512.7 cm^{-1}) and CO (2148.5 cm^{-1}) regions.

After 193 nm photolysis, 20−75% of FA is decomposed (depending on the photolysis time) and some bands appear. Spectrum 1 in Figure 2 shows the result of 193 nm photolysis

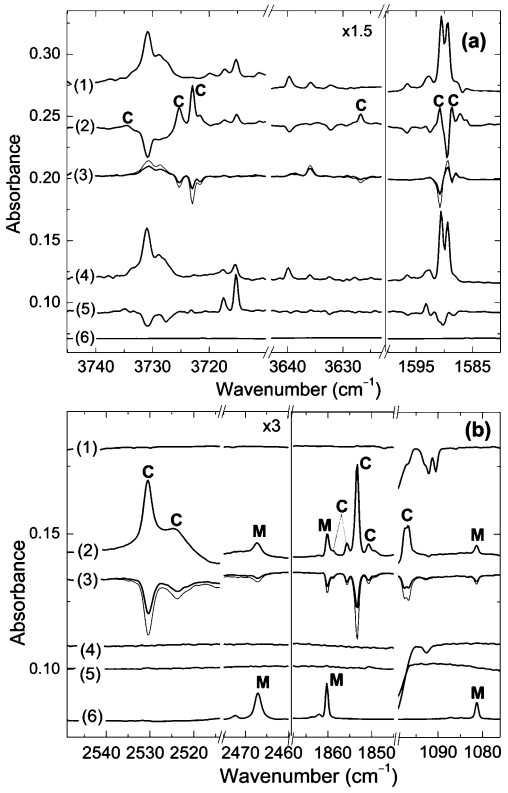

Figure 2. FTIR spectra of the HCO···H_2O complex and related species in a Kr matrix in spectral regions of water (a) and HCO (b). Presented are the difference spectra showing the results of (1) 193 nm photolysis and (2) subsequent annealing of a HCOOH/HBr/Kr (1/2/1000) matrix; (3) 488 nm irradiation of the photolyzed and annealed HCOOH/HBr/Kr matrix for 10 min (thick line) and 35 min (thin line), respectively; (4) 193 nm photolysis and (5) subsequent annealing of a HCOOH/Kr (1/1000) matrix; (6) annealing of a photolyzed CO/HBr/Kr matrix. The annealing temperature was 30 K. The spectra were measured at 4.3 K. The bands of the HCO···H_2O complex and HCO monomer are marked by **C** and **M**, respectively.

(1500 laser pulses) of a HCOOH/HBr/Kr (1/2/1000) matrix, which decomposes about 30% of FA. In the water stretching region, two groups of bands rise at 3730.8, 3728.8, 3717.4, and 3715.4 cm^{-1} and at 3639.8, 3636.0, 3632.5, and 3620.6 cm^{-1}. In the water bending region, two doublets appear at 1596.6/1592.6 cm^{-1} and 1590.4/1589.4 cm^{-1}. In the CO stretching region (not shown), four major bands are observed at 2145.0, 2140.8, 2135.5, and 2130.0 cm^{-1}. All these bands are also formed upon photolysis of a HCOOH/Kr (1/1000) matrix (without HBr, spectrum 4 in Figure 2), and they belong to the CO···H_2O complex, the main photolysis product of formic acid.[34] The CO_2···H_2 complex is also found (asymmetric stretching mode at 2341.6/2340.4/2338.7 cm^{-1} and bending mode at 660.3 cm^{-1}).[34] All bands observed after photolysis of HCOOH are collected in Table S5. Photodecomposition of HBr is more efficient than that of FA, and the HBr absorptions decrease in intensity by ca. 85% after 1500 laser pulses. As a result, H and Br atoms are isolated in the matrix. Bromine atoms absorb in a Kr matrix at 3662 and 3696 cm^{-1} due to the spin−orbit transition ($^2P_{1/2} \leftarrow {}^2P_{3/2}$).[44] The $KrHKr^+$ bands are observed at 1007.6 and 852.5 cm^{-1}.[45] Another minor photoproduct is Br···HBr (2500.6 cm^{-1}) formed from HBr dimers.[46] In the case of HCOOH/HCl/Kr matrices, only ca. 20% of HCl is decomposed after 1500 laser pulses, producing H and Cl atoms, Cl···HCl (2831.5 cm^{-1}),[46] and $KrHKr^+$. The less efficient photodecomposition of HCl is probably due to self-limitations of the photolysis.[47]

Thermal annealing at about 30 K activates mobility of H atoms in a Kr matrix, and they can participate in diffusion-controlled reactions as discussed elsewhere.[48] Annealing of photolyzed HCOOH/HBr/Kr matrices leads to the formation of two absorbers (marked by **M** and **C** in spectrum 2 in Figure 2). Absorber **M** has bands at 2467.1, 1860.3, and 1081.2 cm^{-1} and absorber **C** has bands at 2530.5, 2523.8, 1858.8, 1855.6, 1853.3, 1850.6, and 1097.7/1096.6 cm^{-1}. In the water stretching and bending regions, only bands of absorber **C** (3734.6, 3725.3, 3723.1, 3627.8/3626.8, 1590.7, and 1588.4 cm^{-1}) are observed. These two absorbers are formed synchronously during annealing, but the bands of absorber **C** are much stronger than those of absorber **M**; thus, absorber **C** is supposed to be the main annealing product. These two species are also found in similar experiments with HCOOH/HCl/Kr matrices, but absent after photolysis and annealing of HCOOH/Kr matrices (spectrum 5 in Figure 2). The amount of the CO···H_2O complex monomer decreases upon annealing. It should be noted that the CO···H_2O bands at 3717.4/3715.4 and 3620.6 cm^{-1} somewhat increase upon annealing whereas the bands at 3730.8/3728.5 and 3639.8/3636.0/3632.5 cm^{-1} efficiently decrease. A similar behavior was also observed for photolyzed HCOOH/Kr matrices and this was explained by annealing-induced relaxation of the matrix sites.[34] HBr monomer and HBr dimer are partially recovered by annealing (by ca.15%), and the bands of Br···HBr (2500.5 cm^{-1}) and $BrHBr^-$ (1000.3, 844.9, and 683.2 cm^{-1})[49] increase in intensity. In the case of HCOOH/HCl/Kr matrices, $ClHCl^-$ (915.6 and 662.8 cm^{-1})[49] and HKrCl (1496.5 and 1476.1 cm^{-1})[50] are observed after annealing.

The experiments with CO/HBr/Kr matrices distinguish absorbers **M** and **C**. The IR bands of absorber **M** are strong after photolysis and annealing of these matrices, whereas the bands of absorber **C** are not present (spectrum 6 in Figure 2). Based on this observation, absorber **M** is assigned to the HCO monomer formed via the H + CO reaction. The HCO bands observed in the present experiments (2467.1, 1860.3, and 1081.2 cm^{-1}) are from the CH stretching, CO stretching, and HCO bending modes, respectively, in agreement with previous reports on HCO in neon,[18] argon,[21] krypton,[51] and xenon[51] matrices. The small amount of absorber **M** observed in the HCOOH/HBr/Kr matrices indicates the production of some CO monomer upon photolysis of HCOOH, although its absorption band (2135.7 cm^{-1}) is overlapped with one of the CO···H_2O complex bands (2135.5 cm^{-1}). This suggests a limited cage effect for water and/or CO molecules in 193 nm photolysis of HCOOH in a Kr matrix.

Irradiation at 488 nm efficiently decomposes absorbers **M** and **C** (spectrum 3 in Figure 2), while HCOOH and HBr remain stable. After 488 nm irradiation for 10 and 35 min, ca.

dx.doi.org/10.1021/jp4009477 | J. Phys. Chem. A 2013, 117, 4385−4393

30% and 70% of absorbers **M** and **C** are decomposed, which is accompanied by a recovery of the CO monomer and the CO···H_2O complex consumed by annealing. In addition, HKrCl (in experiments with HCl) is also decomposed by 488 nm light, the amount of $BrHBr^-$ (or $ClHCl^-$) slightly increases, and the amount of CO_2···H_2 is not changed much.

Absorber **C** has not been previously reported in the literature to our knowledge. This species contains water as judged by the presence of the bands in the water stretching and bending regions. In addition, three groups of bands of this absorber are close to the fundamental bands of the HCO monomer so that HCO is a probable part of this species (see Table 2). Figure 3

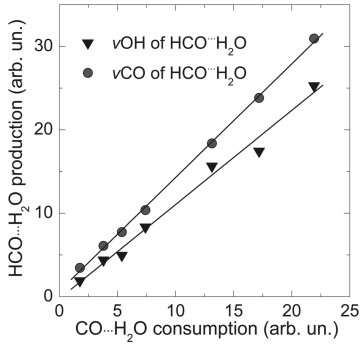

Figure 3. Formation of the HCO···H_2O complex (changes of the νOH bands at 3725.3/3723.1 cm^{-1} and the νCO bands at 1855.6/1853.3 cm^{-1}) as a function of the consumption of the CO···H_2O complex (changes of the νOH bands at 3730.8, 3728.8, 3717.4, and 3715.4 cm^{-1}) upon annealing of a photolyzed HCOOH/HBr/Kr (1/2/1000) matrix at 30 K. The data points correspond to different experiments.

shows the relative amount of absorber **C** as a function of the annealing-induced loss of the CO···H_2O complex. The nearly linear relation between these values suggests that absorber **C** is the HCO···H_2O complex formed in the annealing-induced H + CO···H_2O reaction. In agreement with this assignment, photodecomposition of this new absorber at 488 nm leads to the corresponding recovery of the CO···H_2O complex.

The experiments with DCOOH/HBr/Kr matrices confirm the assignment of absorber **C** to the HCO···water complex. After 193 nm irradiation of a DCOOH/HBr/Kr (1/2/1000) matrix, a number of bands are observed in the OH stretching region at 3691.3, 3687.7, 3685.3, and 3680.0 cm^{-1}, in the OD stretching region at 2709.4, 2704.2, 2693.2, and 2687.8 cm^{-1}, and in the HOD bending region at 1403.1, 1401.1, 1400.0, 1398.6, 1397.0 cm^{-1} (spectrum 1 in Figure 4). This complex also has four characteristic bands in the CO stretching region (not shown), with small frequency shifts relative to the CO···H_2O complex. All these bands are also formed upon photolysis of a DCOOH/Kr (i.e., without HBr, spectrum 4 in Figure 4). These bands were previously observed after photolysis of DCOOH and assigned to the CO···HOD complex.[34] The CO···HOD bands at 3680.0 and 2687.7 cm^{-1} somewhat increase upon annealing (spectra 2 and 5 in Figure 4), whereas the bands at 3691.3/3687.7/3685.3 and 2709.4/2704.2/2693.2 cm^{-1} decrease, which can be explained by annealing-induced relaxation of the matrix sites similarly to the case of the CO···H_2O complex. The minor photoproduct CO_2···HD is also found at 2341.3/2340.3/2338.6 and 660.3 cm^{-1}.[34] All absorptions observed after photodecomposition of DCOOH are collected in Table S5.

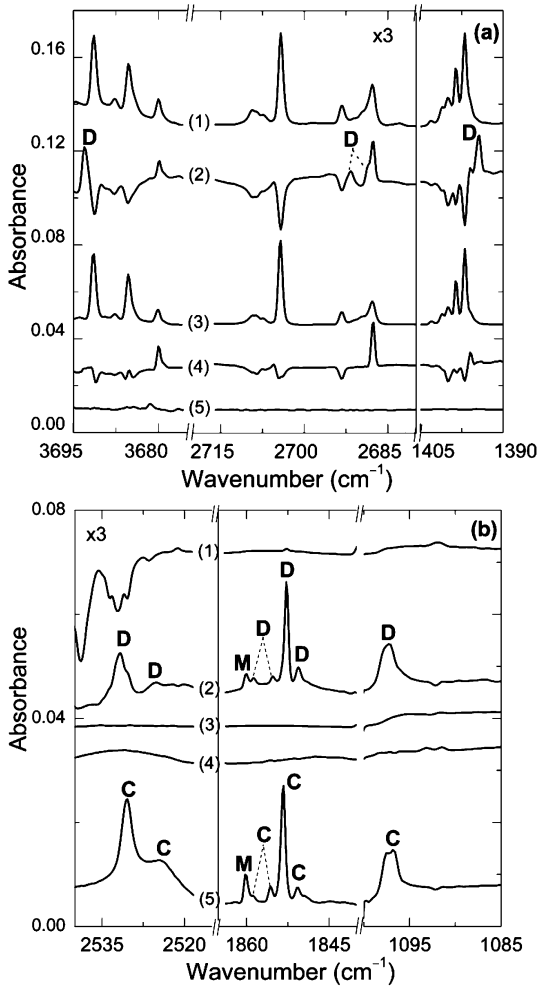

Figure 4. FTIR spectra of the HCO···HOD and HCO···H_2O complex in a Kr matrix in the spectral regions of HOD (a) and HCO (b). Presented are the difference spectra showing the results of (1) 193 nm photolysis and (2) subsequent annealing of a DCOOH/HBr/Kr (1/2/1000) matrix; (3) 193 nm photolysis and (4) subsequent annealing of a DCOOH/Kr (1/1000) matrix; (5) annealing of a photolyzed HCOOH/HBr/Kr (1/2/1000) matrix. The annealing temperature was 30 K. The spectra were measured at 4.3 K. The bands of the HCO···HOD and HCO···H_2O complexes and HCO monomer are marked by **D**, **C**, and **M**, respectively.

Annealing of photolyzed DCOOH/HBr/Kr matrices leads to new absorbers marked by **D** (spectrum 2 in Figure 4). The bands at 3693.0, 2691.6/2688.5, and 1394.5 cm^{-1} are assigned to the OH stretching, OD stretching, and HOD bending modes of the HCO···HOD complex. The bands of absorber **D** at 2531.8/2524.8, 1858.7/1855.1/1852.7/1850.5, and 1097.9/1097.0 cm^{-1} display only minor frequency shifts (ca. <1 cm^{-1}) relative to the HCO···H_2O complex, and these can be assigned to the CH stretching, CO stretching, and HCO bending modes of the HCO···HOD complex (Table 3).

DISCUSSION

The characteristic frequencies of the calculated structures of the HCO···H_2O complex are compared with the experimental results in Table 2. The structural assignment of the observed bands is not straightforward because many of the calculated shifts are similar for the different structures. However, the analysis shows that the strongest bands most probably belong

dx.doi.org/10.1021/jp4009477 | J. Phys. Chem. A 2013, 117, 4385−4393

to structure **III**. The experimental shifts of the CH stretching (+63.4 and +56.7 cm^{-1}) and HCO bending (+16.5 and +15.4 cm^{-1}) mode of structure **III** are in good agreement with the calculated values of +64.9 and +17.5 cm^{-1}, respectively. In the C═O stretching region, four bands are observed (see Figure 2), which fit in principle all structures that have similar calculated shifts from the HCO monomer (from −3.4 to −11.1 cm^{-1}). The intensity ratio of these bands changes in different experiments, indicating the presence of two or more species. When the bands at 1855.6 and 1853.3 cm^{-1} increase in intensity, the bands at 1858.8 and 1850.6 cm^{-1} become smaller (Figure 5a). The intensities of the bands assigned to structure **III** correlate with each other as shown in Figure 5b for the OH stretching mode (3725.3 and 3723.1 cm^{-1}) and the CO stretching mode (1855.6 and 1853.3 cm^{-1}). The present assignment is also confirmed by similar bleaching of these bands upon 488 nm irradiation. The intensities of weaker bands at 3734.6, 1858.8, and 1850.6 cm^{-1} do not correlate with the strongest bands but correlate with each other, indicating that they probably originate from structure **II**. Computationally, structures **II** and **III** are the strongest structures of the $HCO^{\cdots}H_2O$ complex. No evidence of the weakest structure **I** is found in our experiments. Very tentatively, a weak band at 1858.8 cm^{-1} may originate from this structure based on the smallest spectral shift from the monomer.

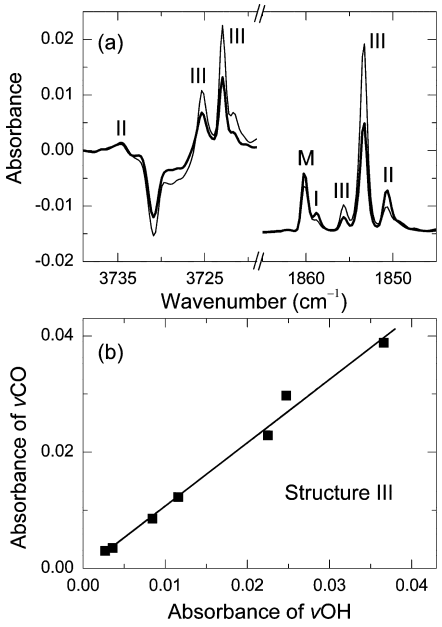

Figure 5. (a) FTIR spectra of the $HCO\cdots H_2O$ complexes in the OH and CO stretching region in two experiments; (b) correlation of the absorbance of the CO stretching mode (1855.6 and 1853.3 cm^{-1}) and the OH stretching mode (3725.3 and 3723.1 cm^{-1}) of structure **III**. The data points correspond to different experiments. The spectra were measured at 4.3 K.

At first glance, it seems that the asymmetric OH stretching bands of the $HCO\cdots H_2O$ complex do not fit any of the calculated structures (Table 2). However, the direct comparison of experiment and theory is complicated by the matrix effect,[51] which changes the band positions of the monomers with respect to vacuum. It follows that the spectral shifts of the complexes in solid matrices can substantially differ from the values calculated in vacuum. As a relevant example, the spectral shifts for HCl upon complexation with N_2 are −14 cm^{-1} by calculations,[52] −8 cm^{-1} in the gas phase,[53] and −2, 0, +6 cm^{-1} in Ar,[54] Kr,[55] and Xe matrices.[56] Similarly, in the case of the $HCO\cdots H_2O$ complex, the OH stretching absorptions of water in a Kr matrix should be at higher frequencies than expected based on calculations. This explains why we may assign the band at 3734.6 cm^{-1} (experimental shift +11.1 cm^{-1}) to structure **II** (calculated shift −2.7 cm^{-1}) and the bands at 3725.3 and 3723.1 cm^{-1} (experimental shifts +2.2 and −0.4 cm^{-1}) to structure **III** (calculated shift −11.3 cm^{-1}). In this case, the experimental interval between these bands (∼10 cm^{-1}) is in good agreement with the calculated value for structures **II** and **III** (8.6 cm^{-1}) rather than for structures **I** and **III** (0.7 cm^{-1}).

The experiments with DCOOH/HBr/Kr matrices confirm the formation of the HCO complex with water and the assignment of the strongest bands to structures **III**. The method of preparation entirely should lead to the $HCO\cdots HOD$ complex (but not to $DCO\cdots H_2O$). Indeed, the $HCO\cdots HOD$ complex is formed by the reaction of an H atom released from HBr and the $CO\cdots HOD$ complex originating from photolysis of DCOOH. This is exactly what was observed in the experiment, i.e., no indication of DCO was found in the spectra. After photolysis and annealing, the CO stretching band of HCO monomer at 1860.3 cm^{-1} is at the same position as previously, whereas the CO stretching bands assigned to the $HCO\cdots HOD$ complex display small but distinguishable red shifts, which supports the deuteration of the water subunit.

The shifts of the HOD bands shed light on the structure of the complex. In experiments, the OH stretching band is blue-shifted by about 16 cm^{-1} from the monomeric value whereas the OD stretching band is red-shifted by about 9 cm^{-1}. As discussed earlier, these experimental values are somewhat influenced by the matrix effect, and the comparison with theory is not straightforward. However, it is important to notice that the difference between νOH and νOD in the complex is increased by ca. 25 cm^{-1} with respect to the HOD monomer, and this value should not be affected much by the matrix effect. Moreover, from the case of $HCO\cdots H_2O$, we have learned that the water stretching modes in the matrix show "more positive" shift than predicted by theory. It follows that the calculated νOH shift of the experimental structure is expected to be small (slightly positive), and the calculated νOD shift should be substantially negative. The calculations show that structures **I** and **III** with the bridging D atom satisfy these requirements whereas structure **II** has very different shifts of the water stretching bands (small and similar). In agreement with the previous conclusions, we assign the observed bands to structure **III** because it is substantially stronger than structure **I**. In this structure **III**, the hydrogen bond is formed by interaction of the O atom of HCO with the D atom of HOD, and the H atom of HOD is terminal. The assigned configuration is in agreement with the calculations and experiments of other HOD complexes, where hydrogen bonding via the D atom leads to bigger binding energy.[57] The preferable interaction with HOD via the D atom is explained by smaller zero-point vibrational energy in this structure. The interaction energy corrected by the zero-point vibrational energy (E_{int}^{CP}+ΔZPVE) confirms that structure **III** with the bridging D atom (−1.94 kcal mol^{-1}) is stronger than that with the bridging H atom (−1.79 kcal mol^{-1}) (see Table 1).

The small shifts of the HCO bands in the $HCO\cdots HOD$ complex (versus the $HCO\cdots H_2O$ complex) are not explained

dx.doi.org/10.1021/jp4009477 | J. Phys. Chem. A 2013, 117, 4385−4393

by our calculations. In the experiments, the partial deuteration of water leads to small blue shifts of νCH and δHCO and a small red shift of νCO. In fact, none of the calculated structures agrees with these experimental shifts even qualitatively. For example, in all calculated structures, the deuteration leads to a decrease of δHCO (Table 3), which disagrees with the experiment. It should be noted in this respect that HCO is an open-shell species, and the accuracy of its description is limited within the used theory. More sophisticated approaches are needed to accurately simulate the absorption spectra of radicals as we did, for example, for CCF radical.[58]

In general, structural assignments of matrix-isolated complexes should be considered with caution. The complex is accommodated in a solid matrix, which can change the complex structure and hence the spectra from those calculated in vacuum. Intuitively, a solid matrix can also change the relative interaction energies of different structures. Practically this means that improvement of the computational level for a complex in vacuum does not necessarily provide a more confident assignment because matrix effects may have a greater contribution to the found discrepancy. Calculation of the HCO···H_2O complex in a large Kr cluster at a good level of theory is a complicated theoretical task, which exceeds the scope of the present work.

A number of additional products are in principle possible in these experiments but not observed. Formaldehyde (H_2CO) can be formed in the H + HCO reaction. The strongest bands of H_2CO in gas phase are at 2843 and 1746 cm^{-1}.[59] No bands in these regions were found after photolysis and annealing of HCOOH/HY/Kr matrices. Only tiny bands at 2810.3 and 1739.0 cm^{-1} were observed in a CO/HBr/Kr (1/2/1000) matrix, which can be assigned to the CH_2 asymmetric stretching and CO stretching modes of H_2CO in a Kr matrix. Isoformyl (COH) radical, which is an isomer of HCO, should also be taken into account[23] In our experiments, no bands suitable for COH were found.

CONCLUSIONS

The complex between HCO and water is characterized by IR spectroscopy in a Kr matrix and by ab initio calculations. In order to prepare this complex, photolysis and annealing of HCOOH/HY/Kr (Y = Br and Cl) matrices are used. Photolysis of HCOOH and HY produces the CO···H_2O complex and H atoms isolated in a Kr matrix. Annealing at about 30 K mobilizes the H atoms and promotes the diffusion-controlled H + CO···H_2O reaction, which leads to the formation of the HCO···H_2O complex. All fundamental absorptions of the HCO···H_2O complex are observed in the experiment exhibiting distinct shifts from the HCO and H_2O monomers.

The calculations at the UCCSD(T)/aug-cc-pVTZ level of theory predict three stable structures of the HCO···H_2O complex (Figure 1). Analysis of the spectroscopic data indicates that the main product has structure **III** stabilized by the intermolecular C−H···O and O−H···O bonds. The formation of structure **II** where the water O atom interacts with the H atom of HCO is less efficient and the experiments give no evidence of the weakest structure **I**. In the experiments with DCOOH, the HCO···HOD complex has structure **III**, in which the hydrogen bond is formed by the D atom. The complexation-induced shifts of the HOD bands are reasonably described by the calculations. In contrast, the very small differences of the HCO band positions between the HCO···H_2O and HCO···HOD complexes are not described by the calculations, which may be connected with limitations of the theoretical description of the open-shell species.

Our results show that the presence of water does not prevent the H + CO reaction, and this reaction still has a low barrier. Thus, HCO can be formed in the presence of water, possibly at water droplets. In fact, the possibility of an increase of this reaction barrier has been considered in the literature.[60] The spectroscopic characterization of the HCO···water complex performed in the present work will hopefully help its identification in the gas-phase experiments, for example, in jets, by IR spectroscopy. The structure of the HCO···water complex is the starting point of the theoretical investigation of chemical reactivity of this complex. Our structural analysis confirms an important conclusion that hydrogen-bonded complexes involving HOD are preferably formed by the D atom.

Photolysis of proper precursors in a matrix has been shown to be an efficient way to produce novel intermolecular complexes.[31−34] The present work uses an advanced "double photolysis" approach combined with thermal annealing. First, two precursors isolated in solid matrix are photolyzed simultaneously producing a small fragment (H atom) and a complex (CO···H_2O). Second, thermal mobilization of the small fragment leads to a chemical reaction with the complex producing a new complex (HCO···H_2O). We believe that other interesting complexes can be formed using this methodology.

ASSOCIATED CONTENT

Supporting Information

The calculated bond lengths of the HCO···H_2O complex (Table S1), calculated vibrational spectra of the HCO···H_2O (Table S2) and HCO···HOD (Table S3) complexes, IR spectra of HCOOH and DCOOH in a Kr matrix (Table S4), IR spectra of the CO···H_2O and CO···HOD complexes in a Kr matrix (Table S5), and complete refs 38 and 39. This material is available free of charge via the Internet at http://pubs.acs.org.

AUTHOR INFORMATION

Corresponding Author

*E-mail: leonid.khriachtchev@helsinki.fi.

Notes

The authors declare no competing financial interest.

ACKNOWLEDGMENTS

The work was supported by the Academy of Finland (Grant code 1139425) and the National Center for Research and Development of Poland (grant ERA-CHEMISTRY-2009/01/2010). The Wroclaw Center for Networking and Supercomputing and the CSC−IT Center for Science in Espoo are acknowledged for allocated computational resources.

REFERENCES

(1) Weber, A., Ed. *Structure and Dynamics of Weakly Bound Molecular Complexes*; Reidel: Dordrecht, The Netherlands, 1987.

(2) Müller-Dethlefs, K.; Hobza, P. Noncovalent Interactions: A Challenge for Experiment and Theory. *Chem. Rev.* **2000**, *100*, 143−167.

(3) Zwier, T. S. The Spectroscopy of Solvation in Hydrogen-bonded Aromatic Clusters. *Annu. Rev. Phys. Chem.* **1996**, *47*, 205−241.

(4) Sennikov, P. G.; Ignatov, S. K.; Schrems, O. Complexes and Clusters of Water Relevant to Atmospheric Chemistry: H_2O Complexes with Oxidants. *Chem. Phys. Chem.* **2005**, *6*, 392−412.

(5) Aloisio, S.; Francisco, J. S. Radical−Water Complexes in Earth's Atmosphere. *Acc. Chem. Res.* **2000**, *33*, 825−830.
(6) Dozova, N.; Krim, L.; Alikhani, M. E.; Lacome, N. Vibrational Spectra and Structures of H_2O−NO, HDO−NO, and D_2O−NO Complexes. An IR Matrix Isolation and DFT Study. *J. Phys. Chem. A* **2006**, *110*, 11617−11626.
(7) Johnsson, K.; Engdahl, A.; Ouis, P.; Nelander, B. A Matrix-Isolation Study of the Water Complexes of Cl_2, ClOCl, OClO, and HOCl and Their Photochemistry. *J. Phys. Chem.* **1992**, *96*, 5778−5783.
(8) Aloisio, S.; Francisco, J. S. A Density Functional Study of H_2O−OClO, $(H_2O)_2$−OClO and H_2O−ClOO complexes. *Chem. Phys.* **2000**, *254*, 1−9.
(9) Ball, D. W. DFT and G2 Calculations on the NO_2−H_2O Molecular Complex. *Chem. Phys. Lett.* **1999**, *312*, 306−310.
(10) Francisco, J. S.; Sander, S. P. Existence of a Chlorine Oxide and Water (ClO−H_2O) Radical Complex. *J. Am. Chem. Soc.* **1995**, *117*, 9917−9918.
(11) Hamilton, E. J.; Lii, R. R. The Dependence on H_2O and on NH_3 of the *Kinetics* of the Self-Reaction of HO_2 in the Gas-Phase: Formation of HO_2−H_2O and HO_2−NH_3 Complexes. *Int. J. Chem. Kinet.* **1977**, *9*, 875−885.
(12) Sander, S. P.; Peterson, M. E. Kinetics of the Reaction HO_2 + NO_2 + M → HO_2NO_2 + M. *J. Phys. Chem.* **1984**, *88*, 1566−1571.
(13) Árnadóttir, L.; Stuve, E. M.; Jónsson, H. The Effect of Coadsorbed Water on the Stability, Configuration and Interconversion of Formyl (HCO) and Hydroxymethylidyne (COH) on Platinum (111). *Chem. Phys. Lett.* **2012**, *541*, 32−38.
(14) Miller, J. A.; Kee, R. J.; Westbrook, C. K. Chemical Kinetics and Combustion Modeling. *Annu. Rev. Phys. Chem.* **1990**, *41*, 345−387.
(15) Herbst, E. The Chemistry of Interstellar Space. *Chem. Soc. Rev.* **2001**, *30*, 168−176.
(16) Woon, D. E. An Ab initio Benchmark Study of the H + CO → HCO Reaction. *J. Chem. Phys.* **1996**, *105*, 9921−9926.
(17) Wang, H. Y.; Eyre, J. A.; Dorfman, L. M. Activation Energy for the Gas Phase Reaction of Hydrogen Atoms with Carbon Monoxide. *J. Chem. Phys.* **1973**, *59*, 5199−5200.
(18) Pirim, C.; Krim, L. A Neon-Matrix Isolation Study of the Reaction of Non-Energetic H-Atoms with CO Molecules at 3 K. *Phys. Chem. Chem. Phys.* **2011**, *13*, 19454−19459.
(19) Sappey, A. D.; Crosley, D. R. Laser-Induced Fluorescence in the B-X System of HCO Radical. *J. Chem. Phys.* **1990**, *93*, 7601−7608.
(20) Cool, T. A.; Song, X. M. Resonance Ionization Spectroscopy of HCO and DCO. II. The B^2A' state. *J. Chem. Phys.* **1992**, *96*, 8675−8683.
(21) Milligan, D. E.; Jacox, M. E. Matrix-Isolation Study of the Infrared and Ultraviolet Spectra of the Free Radical HCO. The Hydrocarbon Flame Bands. *J. Chem. Phys.* **1969**, *51*, 277−288.
(22) Francisco, J. S.; Goldstein, A. N.; Williams, I. H. Dissociation Dynamics of FCO and HCO Radicals. *J. Chem. Phys.* **1988**, *89*, 3044−3049.
(23) Marenich, A. V.; Boggs, J. E. Coupled Cluster CCSD(T) Calculations of Equilibrium Geometries, Anharmonic Force Fields, and Thermodynamic Properties of the Formyl (HCO) and Isoformyl (COH) Radical Specie. *J. Phys. Chem. A* **2003**, *107*, 2343−2350.
(24) Ewing, G. E.; Thompson, W. E.; Pimentel, G. C. The Infrared Detection of the Formyl Radical HCO. *J. Chem. Phys.* **1960**, *32*, 927−932.
(25) Engdahl, A.; Karlström, G.; Nelander, B. The Water-Hydroxyl Radical Complex: A Matrix Isolation Study. *J. Chem. Phys.* **2003**, *118*, 7797−7802.
(26) Langford, V. S.; McKinley, A. J.; Quickenden, T. I. Identification of H_2O−HO in Argon Matrices. *J. Am. Chem. Soc.* **2000**, *122*, 12859−12863.
(27) Nelander, B. The Peroxy Radical as Hydrogen Bond Donor and Hydrogen Bond Acceptor. A Matrix Isolation Study. *J. Phys.Chem. A* **1997**, *101*, 9092−9096.
(28) Mardyukov, A.; Crespo-Otero, R.; Sanchez-Garcia, E.; Sander, W. Photochemistry and Reactivity of the Phenyl Radical−Water System: A Matrix Isolation and Computational Study. *Chem. Eur. J.* **2010**, *16*, 8679−8689.
(29) Wanke, R.; Benisvy, L.; Kuznetsov, M. L.; Guedes da Silva, M. F. C.; Pombeiro, A. J. L. Persistent Hydrogen-Bonded and Non-Hydrogen-Bonded Phenoxyl Radicals. *Chem. Eur. J.* **2011**, *17*, 11882−11892.
(30) Sander, W.; Roy, S.; Polyak, I.; Ramirez-Anguita, J. M.; Sanchez-Garcia, E. The Phenoxyl Radical−Water Complex: A Matrix Isolation and Computational Study. *J. Am. Chem. Soc.* **2012**, *134*, 8222−8230.
(31) Heikkilä, A.; Pettersson, M.; Lundell, J.; Khriachtchev, L.; Räsänen, M. Matrix Isolation and Ab initio Studies of 1:1 Hydrogen-Bonded Complexes HCN−H_2O and HNC−H_2O Produced by Photolysis of Formaldoxime. *J. Phys. Chem. A* **1999**, *103*, 2945−2951.
(32) Pehkonen, S.; Pettersson, M.; Lundell, J.; Khriachtchev, L.; Räsänen, M. Photochemical Studies of Hydrogen Peroxide in Solid Rare Gases: Formation of the HOH−O(^{3}P) Complex. *J. Phys. Chem. A* **1998**, *102*, 7643−7648.
(33) Isoniemi, E.; Khriachtchev, L.; Makkonen, M.; Räsänen, M. UV Photolysis Products of Propiolic Acid in Noble-Gas Solids. *J. Phys. Chem. A* **2006**, *110*, 11479−11487.
(34) Lundell, J.; Räsänen, M. The 193-nm Induced Photodecomposition of HCOOH in Rare-Gas Matrices: the H_2O−CO 1:1 Complex. *J. Phys. Chem.* **1995**, *99*, 14301−14308.
(35) Pehkonen, S.; Marushkevich, K.; Khriachtchev, L.; Räsänen, M.; Grigorenko, B. L.; Nemukhin, A. V. Photochemical Synthesis of H_2O_2 from the H_2O···O(^{3}P) van der Waals Complex: Experimental Observations in Solid Krypton and Theoretical Modeling. *J. Phys. Chem. A* **2007**, *111*, 11444−11449.
(36) Khriachtchev, L.; Domanskaya, A.; Marushkevich, K.; Räsänen, M.; Grigorenko, B.; Ermilov, A.; Andrijchenko, N.; Nemukhin, A. Conformation-Dependent Chemical Reaction of Formic Acid with an Oxygen Atom. *J. Phys. Chem. A* **2009**, *113*, 8143−8146.
(37) Lignell, A.; Khriachtchev, L. Intermolecular Interactions Involving Noble-Gas Hydrides: Where the Blue Shift of Vibrational Frequency is a Normal Effect. *J. Mol. Struct.* **2008**, *889*, 1−11.
(38) Werner, H.-J.; Knowles, P. J.; Knizia, G.; Manby, F. R.; Schütz, M.; Celani, P.; Korona, T.; Lindh, R.; Mitrushenkov, A.; Rauhut, G. et al. *MOLPRO*, v 2010.1, A Package of Ab initio Programs; Cardiff, UK, 2010. See http://www.molpro.net.
(39) Frisch, M. J.; Trucks, G. W.; Schlegel, H. B.; Scuseria, G. E.; Robb, M. A.; Cheeseman, J. R.; Scalmani, G.; Barone, V.; Mennucci, B.; Petersson, G. A. et al. *Gaussian 09*, revision B.01; Gaussian, Inc., Wallingford CT, 2010.
(40) Boys, S. F.; Bernardi, F. The Calculation of Small Molecular Interactions by the Differences of Separate Total Energies. Some Procedures with Reduced Errors. *Mol. Phys.* **1970**, *19*, 553−566.
(41) Weinhold, F. In *Encyclopedia of Computational Chemistry*; Schleyer, P. R., Ed.; John Wiley & Sons: Chichester, 1998; pp 1792−1811.
(42) Lundell, J.; Räsänen, M.; Latajka, Z. Matrix-Isolation FTIR and Ab initio Study of Complexes between Formic Acid and Nitrogen. *Chem. Phys.* **1994**, *189*, 245−260.
(43) Dubost, H. Infrared Absorption Spectra of Carbon Monoxide in Rare Gas Matrices. *Chem. Phys.* **1976**, *12*, 139−151.
(44) Pettersson, M.; Nieminen, J. Spin-Orbit Transitions ($^2P_{1/2}$←$^2P_{3/2}$) of Iodine and Bromine Atoms in Solid Rare-Gases. *Chem. Phys. Lett.* **1998**, *283*, 1−6.
(45) Bondybey, V. E.; Pimentel, G. C. Infrared Absorptions of Interstitial Hydrogen Atoms in Solid Argon and Krypton. *J. Chem. Phys.* **1972**, *56*, 3832−3836.
(46) Lorenz, M.; Kraus, D.; Räsänen, M.; Bondybey, V. E. Photodissociation of Hydrogen Halides in Rare Gas Matrices, and the Effect of Hydrogen Bonding. *J. Chem. Phys.* **2000**, *112*, 3803−3811.
(47) Khriachtchev, L.; Pettersson, M.; Räsänen, M. On Self-Limitation of UV Photolysis in Rare-Gas Solids and some of its Consequences for Matrix Studies. *Chem. Phys. Lett.* **1998**, *288*, 727−733.

(48) Khriachtchev, L.; Saarelainen, M.; Pettersson, M.; Räsänen, M. H/D Isotope Effects on Formation and Photodissociation of HKrCl in Solid Kr. *J. Chem. Phys.* **2003**, *118*, 6403−6410.
(49) Räsänen, M.; Seetula, J.; Kunttu, H. Photogeneration of Ions via Delocalized Charge Transfer States. II. HX_2^- (X═Cl, Br, I) in Rare Gas Matrices. *J. Chem. Phys.* **1993**, *98*, 3914−3918.
(50) Pettersson, M.; Lundell, J.; Räsänen, M. Neutral Rare-Gas Containing Charge-Transfer Molecules in Solid Matrices. I. HXeCl, HXeBr, HXeI, and HKrCl in Kr and Xe. *J. Chem. Phys.* **1995**, *102*, 6423−6431.
(51) Lundell, J.; Jolkkonen, S.; Khriachtchev, L.; Pettersson, M.; Räsänen, M. Matrix Isolation and Ab initio Study of the Hydrogen-Bonded H_2O_2−CO Complex. *Chem. Eur. J.* **2001**, *7*, 1670−1678.
(52) Silvi, B.; Allavena, M. Properties of Monomers in Dimers, an Analysis of Dimerization Effect: Ab initio Calculations on HCl−N_2 and HCl−CO_2 Complexes. *J. Mol. Struct.* **1986**, *135*, 225−233.
(53) Mckellar, A. R. W.; Lu, X. Infrared Spectra of the N_2−HCl and OC−HCl Complexes. *J. Mol. Spectrosc.* **1993**, *161*, 542−551.
(54) Bowers, M. T.; Flygare, W. H. Vibration—Rotation Spectra of Monomeric HCl, DCl, HBr, DBr, and HI in the Rare-Gas Lattices and N_2-Doping Experiments in the Rare-Gas Lattices. *J. Chem. Phys.* **1966**, *44*, 1389−1404.
(55) Lignell, A.; Khriachtchev, L.; Pettersson, M.; Räsänen, M. Large Blueshift of the H-Kr Stretching Frequency of HKrCl upon Complexation with N_2. *J. Chem. Phys.* **2002**, *117*, 961−964.
(56) Khriachtchev, L.; Tapio, S.; Räsänen, M.; Domanskaya, A.; Lignell, A. HY−N_2 and HXeY−N_2 Complexes in Solid Xenon, (Y═Cl and Br): Unexpected Suppression of the Complex Formation for Deposition at Higher Temperature. *J. Chem. Phys.* **2010**, *133*, 084309.
(57) Scheiner, S. Calculation of Isotope Effects from First Principles. *Biochim. Biophys. Acta* **2000**, *1458*, 28−42.
(58) Tarroni, R.; Khriachtchev, L.; Domanskaya, A.; Räsänen, M.; Misochko, E.; Akimov, A. Infrared Spectrum of Elusive C_2F Radical: A Matrix-Isolation and Computational Study. *Chem. Phys. Lett.* **2010**, *493*, 220−224.
(59) Shimanouchi, T. *Tables of Molecular Vibrational Frequencies Consolidated Vol. I*; National Bureau of Standards: Washington, DC, 1972; p 44.
(60) Woon, D. E. Modeling Gas-Grain Chemistry with Quantum Chemical Cluster Calculations. I. Heterogeneous Hydrogenation of CO and H_2CO on Icy Grain Mantles. *Astrophys. J.* **2002**, *569*, 541−48.
(61) Engdahl, A.; Nelander, B. Water in Krypton Matrices. *J. Mol. Struct.* **1989**, *193*, 101−109.